EUROPEAN COMMISSION

Community research

BELBaR

(Contract Number: 295487)

DELIVERABLE (D-N°:3.4)
Report on microscale investigations on colloid mobility controlling processes

Author(s): **V. Petrov, A. Romanchuk (MSU)**
G. Darbha, J. Lützenkirchen, T. Schäfer (KIT-INE)
U. Alonso, T. Missana (CIEMAT)

Reporting period: 01/06/13 – 31/05/14

Date of issue of this report: **02/06/14**

Start date of project: **01/03/12** Duration: 48 Months

Project co-funded by the European Commission under the Seventh Euratom Framework Programme for Nuclear Research &Training Activities (2007-2011)

EURATOM

Dissemination Level		
PU	Public	X
RE	Restricted to a group specified by the partners of the BELBaR project	
CO	Confidential, only for partners of the BELBaR project	

DISTRIBUTION LIST

Name	Number of copies	Comments
Christophe Davies (EC)	One electronic copy submitted via participant portal	
BELBaR participants	One electronic copy available on the BELBaR webportal	

1. Microscale investigation on colloid mobility controlling processes: MSU contribution by Petrov, V., Romanchuk, A.

Thorium dioxide is known to be the easiest representative of actinides dioxides due to its constant stoichiometry and insensitivity to redox conditions. Investigation of nanosized ThO_2 stability in solutions of different pH values and ionic strengths provides the information about migration behavior of other actinide oxides in environment. In this work stability of colloidal suspensions was investigated in terms of ζ-potential dependence on pH. Colloidal particles with high absolute values of ζ-potential are stable and consequently have tendency to migrate. Vice versa colloids with near zero values of ζ-potential have tendency to coagulate and precipitate.

Figure 1 presents data on ζ-potential dependence on pH for suspensions of ThO_2 nanoparticles in solutions of different ionic strengths ($NaClO_4$). Stability of these systems means stability of aggregates and not the single nanoparticles (2 nm).

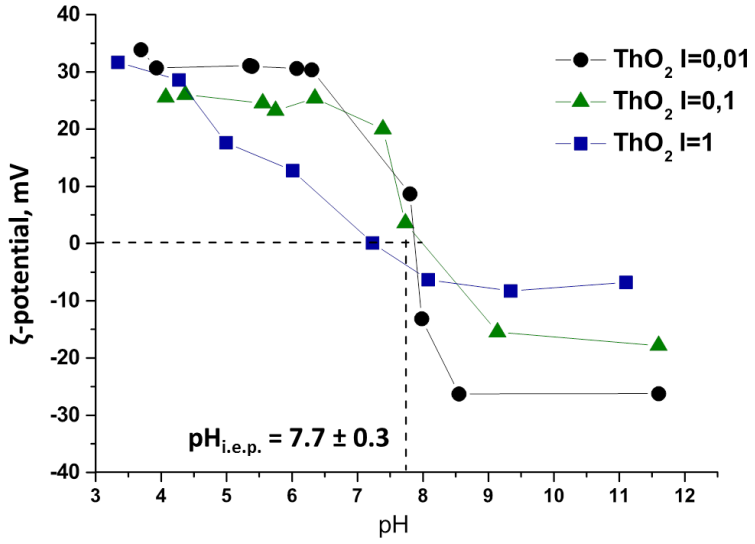

Figure 1. Dependence of ζ-potential on pH values for nanosized ThO_2 suspensions at different ionic strengths.

In all cases the absolute value of ζ-potential is less than 40 mV. The significant decrease of pH range, where colloidal suspensions are stable, is observed with increasing the ionic strength from 0.01 to 1 M. For aggregates the pH range of stability is 3.5÷6.5 and 8.5÷12 in solution of 0.01 M ionic strength. At a tenfold increase in the ionic strength aggregates are stable only in pH range from 4 to 7. In solutions of 1 M ionic strength stability of aggregates can be observed only at pH 3.5÷4.5. The pH value of isoelectric point ($pH_{i.e.p.}$) is found to be

7.7 ± 0.3.

Close value of $pH_{i.e.p.}$ was found for CeO_2 nanoparticles of different size (Figure 2). In this case $pH_{i.e.p.}$ ~ 6.5, and pH range of aggregate stability is 2 ÷ 5; 8 ÷ 10. It has to be mentioned that groundwater in proposed area for future SNF repository in Russia has the ionic strength of values of 1-10 mM and pH 7-8. That means that in these conditions colloidal suspensions of actinide nanoparticles can be (meta)-stable.

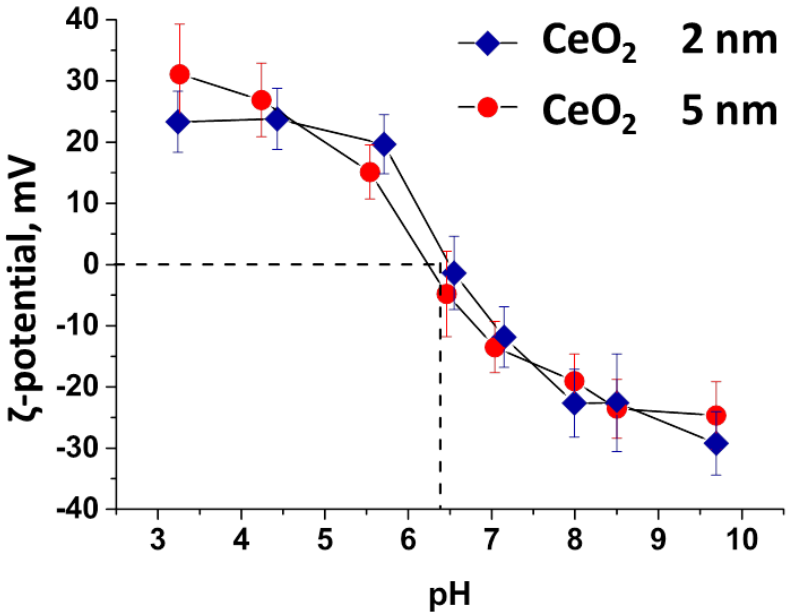

Figure 2. Dependence of ζ-potential on pH values for nanosized CeO_2 suspensions for different particle size.

2. State-of-the art report of the work performed at KIT-INE by Darbha, G., Lützenkirchen, J., Schäfer, T.

Understanding the colloid and rock mineral interaction as a function of solution chemistry ([Eu(III)], pH and ionic strength) and rock surface heterogeneity

Introduction

Bentonite clay is often the recommended back fill material in the context of deep geological radioactive waste disposal. Clay colloids may be generated when groundwater is contact with this geo-engineered barrier. Subjected to their stability, colloids (or colloid associated

radionuclide) can migrate along the micron fractures that are naturally present in the underground systems posing potential threat to contaminate the nearby aquifers. Hence it is important to understand the interaction of bentonite clay colloids with granite (host rock: major constituents are biotite, quartz, plagioclase, K-feldspar) surfaces in the presence of radionuclides. Though retention or transportation of the colloids is primarily governed by chemistry at the interface, the contribution from fluid hydrodynamics and rock surface heterogeneity can add significantly to the mechanism of colloid deposition. A deep study is required to obtain colloid deposition efficiencies as an interplay between various physiological and chemical factors which can be a direct input to the predictive contaminant transport calculations. Structurally, bentonite (the major component is montmorillonite) is made of two basic building blocks: the aluminium octahedral sheet and the silica tetrahedral sheet. Probing aluminol and silanol groups at clay edge sites determining the reactivity and metal ion interaction are a special focus of research. The current topic is focused on a) quantification of colloid deposition efficiencies onto mineral surfaces using Vertical Scanning Interferometry (VSI) as a function of surface roughness under varying [Eu(III)] b) estimation of interaction forces between colloids and mineral surfaces under vaying Eu(III) using Atomic Force Microscopy (AFM).

Deposition of colloids on Granite and its mineral components:

The granodiorite sample is from GTS, Grimsel, Switzerland. It is composed of quartz (15%), plagioclase (28%), K-feldspar (7%), biotite (41%) and clay minerals (0-1%) by volume. The minerals plagioclase, K-feldspar, and quartz minerals were purchased from Dr. F. Krantz GmbH, Bonn, Germany. Biotite mineral was purchased from WARD'S Natural Science, NY, U.S.A. Samples (granodiorite, quartz, plagioclase, K-feldspar and biotite) of approximately 1 x 1 x 0.4 cm^3 were exposed to polystyrene colloids of 1 μm size in an open-fluid cell (flow velocity 0.02 mL/min) for 60 min. The surface topography characterization (roughness parameters: *Rq, Rt, R10z, F*) and colloid quantification (Sherwood number, *Sh*) was done by VSI. The interaction forces between colloids and minerals surfaces was analyzed by AFM using colloid probe technique where a colloidal particle (Al_2O_3 or SiO_2) is attached at the end of AFM cantilever. The in-situ force force measurements were possible using a home-designed fluid cell. Argon was purged into the stock solution and in the AFM chamber continuously throughout the measurements.

a) Influence of surface roughness of granodiorite and Eu(III) concentration on colloid deposition efficiency:

An increase in both roughness (*Rq*) and Eu(III) concentration increased colloid deposition efficiency on granodiorite. In the absence of Eu(III), an increase in *Rq* for surface sections from 450 to 1100 nm showed an increase in *Sh* by a factor of 24 (Ref 1). A large variation in deposition efficiency is predominantly influenced by roughness variations. Half-pores that exist on the rock in-between crystals (intergrannular porosity) has major impact on colloid

retention. An increase in porosity results in enhancement of colloid sorption for [Eu(III)] ≤ 5x 10^{-7} M. Site-specifically, colloid deposition was predominantly along the pore-walls influenced by the sub-micron scaled protrusions (Figure 1). At higher Eu(III) concentrations (≥ 5 x 10^{-7} M), the sorption of colloids is independent of pore volume. This is due to the sorption of Eu(III) to smooth surface portions where $Sh_{smooth\ portions}$ dominates $Sh_{\text{pore volume}}$. The protrusions along half-pores diminish the overall DLVO interaction energy (due to lower contact area between colloids and substrate) between particles and surfaces rendering favorable for deposition. Moreover, the hydrodynamic shear forces acting on the mineral substrate are at maximum adjacent to colloids and reach a minimum along half-pores, i.e. the rear stagnation point. This provides higher collision frequencies due to increased residence time and finally results in enhanced colloid retention. Our study showed that the colloid sorption is clearly favored at surface sections with high density of small asperities (density= 2.6 ± 0.55 μm^{-1}, asperity diameter= 0.6 ± 0.2 µm, height= 0.4 ± 0.1 µm) in contrast to surface sections with larger asperities and lower asperity density (density = 1.2 ± 0.6 μm^{-1}, d = 1.4 ± 0.4 µm, height = 0.6 ± 0.2 µm).

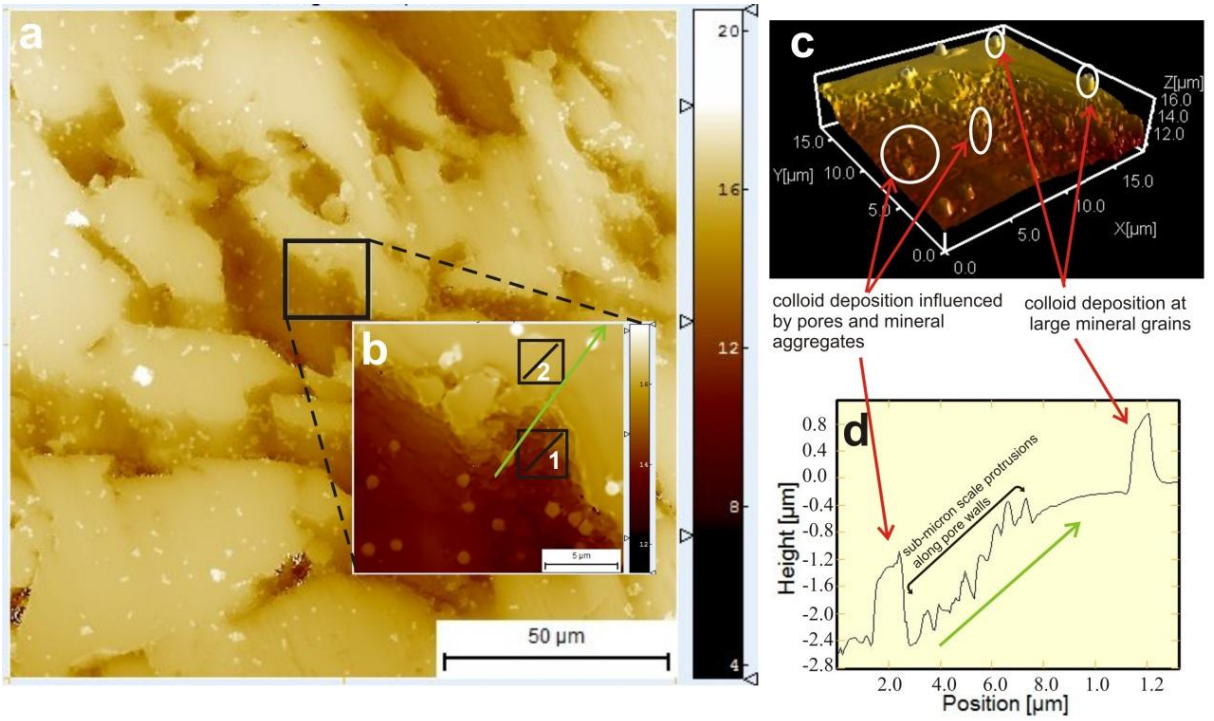

Figure 1. (a) Sites of preferred particle retention at rough granodiorite surface. (a) Map from VSI data showing both flat surface sections and pores; (b) inset shows preferred particle deposition at the pore-walls; (c) three-dimensional view of section (b) illustrates height position of adsorbed particles at pore walls; (d) height profile (see location in (b), green line) showing examples of sites occupied by adsorbed colloids at pore walls with micron- to submicron-sized asperities

b) Interaction forces between colloids and mineral surfaces:

Colloidal probes modified with Al_2O_3 and SiO_2 particles at the end of the AFM cantilever are used to mimic clay edge sites and estimate forces against mineral surfaces (quartz, plagioclase, K-feldspar and biotite) under varying pH and trace metal concentration, here Eu(III) (0 to 10^{-5} M). For each concentration of Eu(III), the force-volume measurements were

obtained at 256 points on the substrate. The average force of adhesion of 256 points is represented as the overall adhesion force between particle and surface (F_{adh}).

i) As function of pH and Eu(III)

The force meausrements were performed at I = 10 mM NaCl and pH 5 and 9. At pH 5, increasing [Eu(III)] from 0 to 10^{-5} M results in an increase of the adhesion force between the SiO_2 particle and the mineral surfaces, except for quartz. A change in [Eu(III)] or pH has shown no such significant changes when using Al_2O_3 particle as a probe. At [Eu(III)]=10^{-5} M, the ratio $F_{adh(SiO2)}/F_{adh(Al2O3)}$ decrease in the order: 11.3 for biotite > 4.55 for plagioclase > 3.03 for K-feldspar > 0.22 for quartz. An increase in pH from 5 to 9 resulted in decrease of adhesion forces by a factor of ~4 - 8 for SiO_2 and ~8 - 12 in the case of Al_2O_3. At pH 9 and at [Eu(III)]=10^{-5} M, the ratio $F_{adh(SiO2)}/F_{adh(Al2O3)}$ decreased in order: 19 for biotite > 6.41 for K-feldspar > 3.38 for plagioclase > 1.64 for quartz.

ii) As function of ionic strength

The force measurements were performed at pH = 5 and varying ionic strength (1 & 10 mM NaCl). As predicted by DLVO theory, a 10 fold increase in ionic strength showed an increase in adhesion forces between colloidal probe and surfaces. A similar trend of adhesion was observed between colloid and mineral surfaces independent of ionic strength. At 10^{-5} M Eu(III), from 1 to 10 mM NaCl the order of adhesion forces for Al_2O_3 are: 5.76 for plagioclase > quartz 3.99 > biotite 2.41 > K-felspar 3.25. In the case of SiO_2 the order is: plagioclase 1.88 > K-feldspar & biotite 1.71 ≈ quartz 0.68. Overall, SiO_2-biotite adhesion forces dominate the remaining colloid-mineral interactions.

iii) As function of surface roughness

Adhesion forces between four different Al_2O_3 colloid probes of similar size (8 μm) against a smooth biotite (Root mean square roughness, *Rq*<1-3 nm) as a function of pH was performed. Though similar trend of adhesion forces was observed with maximum at pH 6, a change in the magnitude of adhesion forces (1.2 to 2 time) was observed, which is attributed to the rough features (of ~10 nm range) along colloidal particle verified by SEM and AFM, which demonstrates the influence of roughness on particle adhesion forces.

Further, the interaction force measurements between colloids and minerals under GGW conditions are planned for the next step. Also, colloid deposition experiments with granitic fracture experiments with varying fracture aperture distance followed by successful model evaluations are a step forward. In parallel, the polymeric replica of the fracture will be considered to eliminate the impact of chemical heterogeneity.

Reference:

1. Darbha, G., Fischer, C., Luetzenkirchen, J., Schäfer, T. (2012) Site-specific retention of colloids at rough rock surfaces. Environmental Science & Technology, 46, 9378

3. CIEMAT contribution (Ursula Alonso, Tiziana Missana)

CIEMAT is studying micro-scale retention of colloids in granite surface by the application of the ion beam techniques *Rutherford Backscattering Spectrometry* and *micro-Particle Induced X-Ray Emission* (μPIXE).

This report summarizes the results on: (A) RBS analyses of the contribution of colloid in-depth access (diffusion) to micro-scale retention in Grimsel granite surface, accounting for the heterogeneity exhibited by the rock minerals in pore distribution and electrostatic charge and (B) μPIXE first analyses of heterogeneous GRismel granite and Äspö diorite.

(A) RBS micro-scale analyses of the of colloid diffusion in Grimsel granite

A1. Introduction

Colloid-driven radionuclide (RN) transport in deep geological repositories (DGR) for high-level radioactive waste is of concern (Geckeis, 2008; Missana et al., 2011; Schaefer et al., 2012). In fractured rocks, colloid transport mainly takes place by advection in the water flow, being greatly affected by different mechanisms that contribute to colloid filtration (Albarran et al., 2011; Missana et al., 2008a). Colloid retention has been observed even at conditions where high retention was not expected, i.e. under unfavorable electrostatic conditions (Missana et al., 2008b; Schäfer et al., 2004). The mechanisms that contribute to colloid retention are not yet understood.

Colloid diffusion in rock matrix can eliminate colloids from the flow paths and despite being considered a minor mechanism, it is often accounted for to interpret the tailing behavior of colloid breakthrough curves in transport experiments (James and Chrysikopoulos, 1999; Kosakowsky, 2004; Möri et al., 2003).

The extent of diffusion is expected to be dependent on rock porosity and pore size and therefore size-dependent, resulting from exclusion caused by the smaller pore spaces or by the existence of tortuous paths. But also, the crystalline rock surface presents a great heterogeneity in their physical and chemical properties, being composed of different minerals. Therefore, heterogeneous electrostatic charge distribution of granite surface could play also a relevant role on colloid diffusion.

The aim of this study is to quantify the diffusion of colloid particles on a heterogeneous granite surface. Analyses are carried out at mineral scale, since a nanoparticle would not be affected by the physicochemical conditions of the average granite surface, but by the specific conditions of a certain mineral, grain boundary, roughness or defect (Song and Elimelech, 1993). The chemical conditions were selected ensuring colloid stability, and at the same time trying cover possible electrostatic interactions with respect to granite minerals.

A2. Materials

The selected colloids were CeO_2, Fe_2O_3 and Au, with different particle size and charge conditions. Cerium oxide nanoparticles (CeO_2) were supplied by AEA Technology with a particle size of 60 nm at pH = 4, according to the supplier. For diffusion studies, the initial suspension (2.05% in weight) was diluted in granitic water of low ionic strength (water composition in Table 1), to a concentration of 100 mg/L. The pH of the CeO2 suspension, diluted in the granite water, was pH = 4.45.

Iron oxide hematite nanoparticles (Fe_2O_3) were supplied by AEA Technology with a particle size of 125 nm, a concentration of 0.1% in weight and pH 6. For diffusion studies the suspensions were diluted in the granitic water (Table 1) to a final concentration of 1000 mg/L. The pH did not vary significantly upon dilution.

Gold colloid suspensions from BBInternational, suspended in pure water and only

containing a residual gold chloride concentration of 0.001 %, of 40 and 100 nm were also selected. The Au suspensions were used without any dilution.

Granite from the FEBEX tunnel at the Grimsel Test Site Underground Laboratory (Switzerland) was selected (Huertas et al., 2000). For diffusion studies granite samples were cut into millimeter-sized slices with an average area of 1 cm^2. The granite surface was polished to standardize surface roughness. The mean porosity measured for this granite was 0.3 %. Typical pore size ranged from 50-200 nm, with some fissures in the micrometer range (Alonso et al., 2003). Granite samples have an average accessible porosity of 0.75 %. Quartz minerals and feldspars showed porosity of 0.5 % while the dark minerals (generally micas and Fe-minerals), which represents about an 8% in volume of the total granite, had higher porosity (> 1.4 %) (Leskinen et al., 2007).

A3.Materials characterization

The size, stability and charge conditions of the selected nanoparticles and the charge of granite minerals were verified to establish the experimental conditions, accounting for all possible electrostatic interactions.

To determine the average hydrodynamic diameter of the colloid suspensions *Photon Correlation Spectroscopy (PCS)* measurements were carried out at different pH conditions. PCS analyses were performed with a 4700 Malvern apparatus equipped with Spectra Physics a 4 W argon laser (λ=514 nm). The angle of scattering was 90°. Coagulation rates of the colloidal suspensions were obtained experimentally by means of time-resolved dynamic light scattering experiments. The particle aggregation was determined, observing the variation of the mean hydrodynamic diameter with time during one hour approximately; the single measurements lasted 60 seconds.

A Malvern Zetamaster equipped with a 5 mW He-Ne laser (λ = 633 nm) was used to measure the zeta potential (ζ) as a function of the pH in diluted (1:25) colloid suspensions. Figure 1 shows the zeta potential measured as a function of pH for studied colloid and for main minerals composing granite, prepared in low mineralized granitic water (Na-HCO_3 type, pH 8.3 and conductivity 282 μS/cm), as a function of pH.

Gold colloids are negatively charged over almost the whole pH range, with an isoelectric point near pH = 3, responsible for the rapid coagulation near this pH. CeO_2 colloids show a positive zeta potential (+ 8 mV) at their initial pH (pH 3). By increasing the pH the potential decreases, with an isoelectric point around pH 6.3. By increasing the pH the zeta potential starts to be negative, with a value around -3 mV. This low potential explains the rapid colloid coagulation observed at basic pH. Potential values for Fe_2O_3 are positive (maximun +50 mV) for pH < 7.5 and negative (-40 mV) at higher pH.

In Figure 1B, the zeta potentials of the granite and its main minerals (feldspar, a mixture of quartz and plagioclase, biotite and also muscovite) are plotted as function of the pH. At all the pHs, the granite surface charge is, in average, negative. The major minerals composing the granite, as quartz-plagioclases or feldspars (70 % of the total granite) present similar negative behavior as the granite. However, dark minerals such as biotite present a point of zero charge at pH 6 to 7. The point of zero charge reported for other Fe minerals are 5.6 for ilmenite (Fan and Rowson, 2000) and 5.5 for chlorite or epidote (Fornasiero and Ralston, 2005). Therefore, all these minerals are positively charged at acidic conditions.

With this information, the experimental conditions for diffusion analyses were fixed, to consider the possible colloid/rock charge interactions. On the rock part, at acid pH conditions minerals with positive and negative charge coexisted, at acid-neutral conditions minerals showed neutral or negative charge and at basic conditions most granite minerals are negatively charged.

From the colloids, the evaluated cases were: (i) zero charge (Au at pH 3), (ii) low positive charge (CeO_2 and Fe_2O_3 at pH 4-5) (iii) high positive charge (Fe_2O_3 at pH 3, (iv) low negative charge (CeO_2 at pH 10) and (v) high negative charge (Au at pH 6). A summary of studied conditiosn is presented in Table 1.

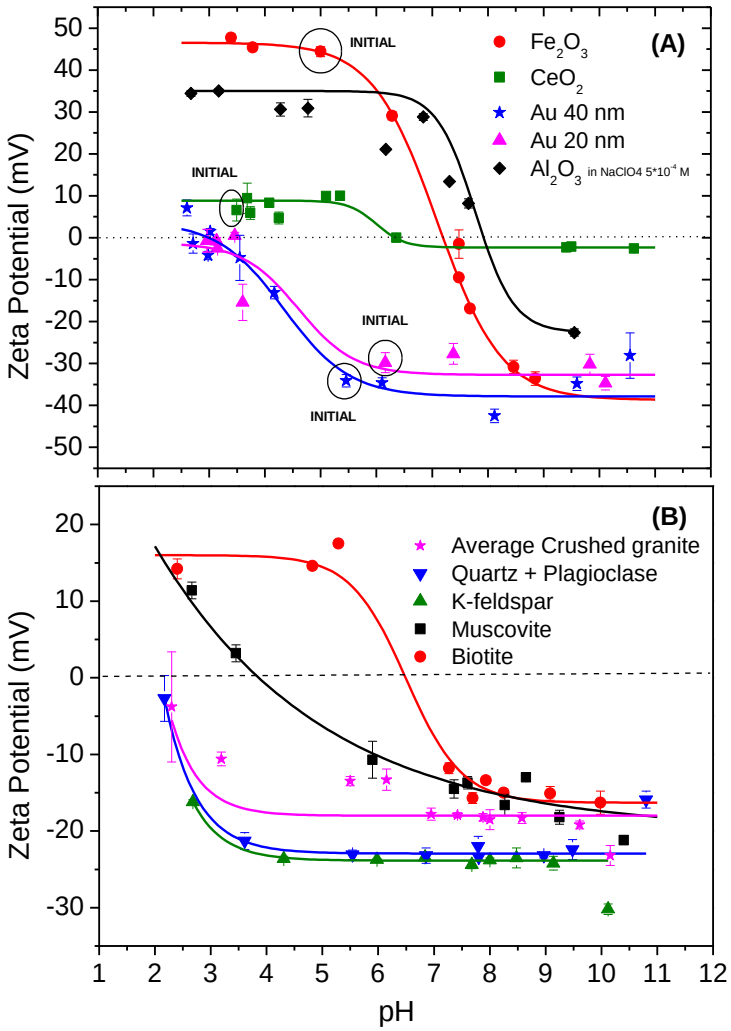

Figure 1. (A) Zeta potential measured as a function of pH for Au colloids (SizeINI= 40 nm at pH6), CeO_2 (SizeINI= 60 nm at pH 3) and Fe_2O_3 colloids (SizeINI= 100 nm at pH 5.28). (B) Zeta portential of main minerals composing granite as a function of pH.

A4.RBS diffusion studies on granite surface at mineral micro-scale

Granite slices, previously saturated in low mineralized granitic water (Na-HCO_3 type, pH 8.3 and conductivity 282 µS/cm), were immersed in the different colloid suspensions and at different pH conditions. Contact times ranged from 5 minutes to 4 days. Before RBS measurements, all the samples were cleaned with ethyl alcohol to avoid the presence of particles deposited on the surface. Cleaning is important because the presence of particles on

the granite surface could bias the real diffusion process (Patelli et al., 2006).

The granite surfaces were analyzed with Rutherford Backscattering Spectrometry (RBS). RBS measurements were made with a HVEC 2.5 MeV Van de Graaff accelerator using 2.2 MeV α- particles with a scattering angle of 20º. All samples were covered with a carbon layer of about 100 Å to avoid electrostatic charge effects during ion beam radiation. Mean acquisition time for a single spectrum was 45 minutes, with an accumulated charge around 100 μC. The typical areas analysed by RBS, upon our experimental conditions, are of $1mm^2$, so that in principle single minerals can be analyses, even if the presence of various minerals cannot be completely ruled out. For that reason the standard composition of the average Aare Grimsel granite have been also analysed.

The RBS application to diffusion studies in granite was deeply described in (Alonso et al., 2007b) where the diffusion of Au colloids of different size (from 2 nm to 250 nm) was analyzed in a Spanish granite. In that previous work, the analyses were performed only on granite "white" minerals, with no Fe- content, generally on plagioclases or k-feldspars at pH 6 so that both the colloids and the granite minerals are negatively charged. In the present study, the analyses are extended to other granite composing minerals.

As example, Figure 2 shows the RBS spectra of granite minerals (biotite and quartz) after contact with CeO_2 colloids at pH 3. Only the spectra in those energies near the region of interest for Ce (1.8-2.0 MeV) are shown. The spectra simulations are also included. At this pH 3, quartz minerals are negatively charged while biotite positively charged (Figure 1). In all all the RBS spectra obtained, the signal of Ce is clearly visible being the Ce peaks asymmetrical, presenting a tail pointing towards lower energies indicating that Ce colloids are penetrating in the granite, and therefore diffusing. However, diffusion length was longer in quartz or feldspar minerals due to attractive interaction.

The same analyses were carried out in all considered cases, and in order to obtain diffusion lengths and diffusion coefficients on selected minerals spectra simulation was carried out as described in (Alonso et al., 2007a).

Table 1 presents a summary of colloid diffusion coefficients measured by RBS for the different colloids on different granite minerals, and at different experimental conditions.

RBS results demonstrated that colloid access in-depth was equivalent in all cases, independently of the electrostatic interactions, so that it is mainly conditioned by colloid to pore sizes ratio and limited, since the colloid concentration inside rock was similar, independently of the colloid nature or the initial colloid concentration (from 50 to 1000 ppm).

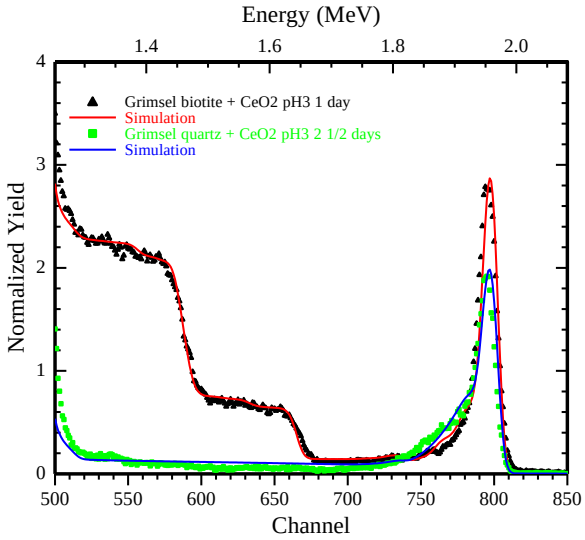

Figure 2. RBS spectra of granite minerals (biotite and quartz) after contact with CeO_2 colloids at pH 3. The spectra simulations are also included.

Table 1. Colloid diffusion coefficients measured by RBS on different granite minerals at different experimental conditions.

Colloid	Size (nm)	pH	Colloid Zeta Potential (mV)	Mineral Zeta potential (mV)	Diffusion coeficcient D_a (m^2/s)
Au	20	6.2	-35 mV	Feldspar: -25 mV	$(2.0 \cdot \pm 0.1) \cdot 10^{-18}$
Au	20	6.2	-35 mV	Biotite: +15 mV	$(4.7 \cdot \pm 0.1) \cdot 10^{-18}$
Au	20	9.0	-30 mV	Feldspar: -25 mV	$(1 \cdot \pm 0.1) \cdot 10^{-18}$
Au	20	9.0	-30 mV	Biotite: -15 mV	$(3.4 \cdot \pm 0.1) \cdot 10^{-18}$
CeO_2	60	3.0	+8 mV	Quartz: -15 mV	$(4.7 \cdot \pm 0.1) \cdot 10^{-18}$
	60	3.0	+8 mV	Feldspar: -15 mV	$(4.3 \pm 0.1) \cdot 10^{-18}$
	60	3.0	+8 mV	Biotite: +15 mV	$(1.9 \cdot \pm 0.1) \cdot 10^{-18}$
Fe_2O_3	60	4.5	+20 mV	Mica: -12 mV	$(7.9 \cdot \pm 0.5) \cdot 10^{-18}$
Fe_2O_3	60	4.5	+20 mV	Quartz: -15 mV	$(3.6 \cdot \pm 0.5) \cdot 10^{-18}$

A5.Conclusions

Colloid diffusion coefficients have been measured, for several sized and charged colloids, in different minerals in natural granite. All diffusion coefficients (Da) measured were in the range of 10^{-18} m^2/s. No significant differences in colloids Da were observed amongst colloid of different charge, but the main differences were attributed to size variations.

Diffusion results indicated that, in order to complete micro-scale colloid retention studies,

accounting for rock heterogeneity in terms of electrostatic charge, to determine colloid surface distribution coefficients (Ka) in granite, at a mineral scale is still required.

(B) µPIXE micro-scale analyses on Grimsel granite and Äspö diorite

B1.. Introduction

CIEMAT aim within this WP is to quantify colloid retention on heterogeneous rock surface. This section presents the micro – Particle Induced X- Ray Emission (µPIXE) analyses that are being carried out to determine colloid surface distribution coefficients (Ka) at mineral micro-scale.

In the past, we analyzed colloid retention on granite surface as a function of colloid size, with Au colloids of different size (Alonso et al., 2009). Main analyses are being carried out at the micro-scale facility of the AN2000 accelerator at the Legnaro National Laboratories of the INFN (Padova, Italy).

At present, the evaluation of colloid/rock electrostatic interactions requires further analyses. In particular, to accounts for all possible colloid /surface interactions, experiments have to be carried out with colloid composed by elements easily detected in the rocks (Alonso et al., 2004). In that sense, rock composition has to be determines as precise as possible, applying the same methodology used for diffusion analyses.

With that purpose, rock samples form Grimsel (Switzerland) and Äspö (Sweden) hard rock laboratories were analyzed by PIXE at the AGLAE external micro-beam line at the C2RMF (Louvre Museum, France) (Moignard et al., 2012). At present, AGLAE counts with a new detection system attached to external micro-beam multipurpose beamline with a high spatial resolution performance, beam stability and capability of multi-technique.

Geological materials are highly heterogeneous and consequently the retention of colloids and contaminants is heterogeneous as well. In this frame, the capabilities of the new AGLAE set-up would allow an improved characterization of natural heterogeneous rock, detecting the presence of the elements of interest at concentration levels of tens of ppm. This provides a better characterization of the initial system, avoiding biased interpretation of colloid retention properties. Additionally, if lower detection limits were achieved, new perspectives to evaluate retention of low solubility contaminants in a wider range of geochemical conditions would be opened.

In this report, first characterization experiments carried out on Grimsel (Switzerland) and Äspö to determine elemental minimum detection limits (MDL) in these samples are presented here and have been partially included in (Zucchiatti et al., In press).

B2.. Materials

Granite discs of around 11.8 mm in diameter and 1 mm thick were cut from a cylindrical sample extracted from a granite block (granodiorite type) coming from the FEBEX gallery located at the Grimsel Test Site Underground Research Laboratory (Switzerland) (Bradbury, 1989) Diorite samples came from the Äspö (Sweden) underground research laboratory (Sundberg, 2002) and they were handled, transported and stored under anoxic conditions (KIT-INE, 2011).

B3. Experimental set-up

Natural rock samples (Grimsel and Äspö), were scanned by PIXE at the New-AGLAE detection system, to test measurement protocols and assess the minimum detection limits (MDL) in the samples, and allowed by the five detectors system.

The main features of the new AGLAE set-up can be found in (Moignard et al., 2012; Zucchiatti et al., In press). The system has a multi detector system that allows full mapping

capability in air, assisted by a powerful event by event reconstruction software. These features allow lower Minimum Detection Limits (MDL) which should be advantageous for the detection of elements that are present in geological, archaeological to the level of a few tens ppm.

Rock samples were irradiated with 3 MeV protons over a surface of 1.920x1.920 mm^2, with the configuration 1LE+4HE (the low energy detector and four filtered -50 mm Al-detectors, summed). Dose-equivalent of 10 Mcts and current-equivalents from 4 to 7 Kcts/sec were used. These corresponded to individual detector count rates of up to 40 Kc/sec.

The PIXE spectra were deconvoluted by the GUPIX program (Campbell et al., 2000) assuming that all the elements were in oxide form and that the target was infinitely thick and the concentration sum was 100%. The four high energy spectra have always been added before deconvolution, but in several cases also individual high energy spectra have been analyzed. The oxide composition has been obtained by combining the results of low and high energy detectors with an already established procedure (Zucchiatti et al., 2002). Taking advantage of the mapping capability (electrostatic + mechanical) and the high sensitivity of the detection system, we have selected map regions corresponding to specific minerals with MapPIXE acquisition and processing system (Pichon et al., 2010) and the corresponding PIXE spectra have been analyzed using the same procedure.

B4. Results

Several granite samples were scanned with the configuration 1LE+4HE and elemental concentrations and MDL's were extracted from the PIXE spectra produced by the whole scanned area.

Figure 3, presents an example of the µPIXE elemental maps obtained on a region selected on an Aspö diorite sample. From this type of mas, the elemental composition can be derived.

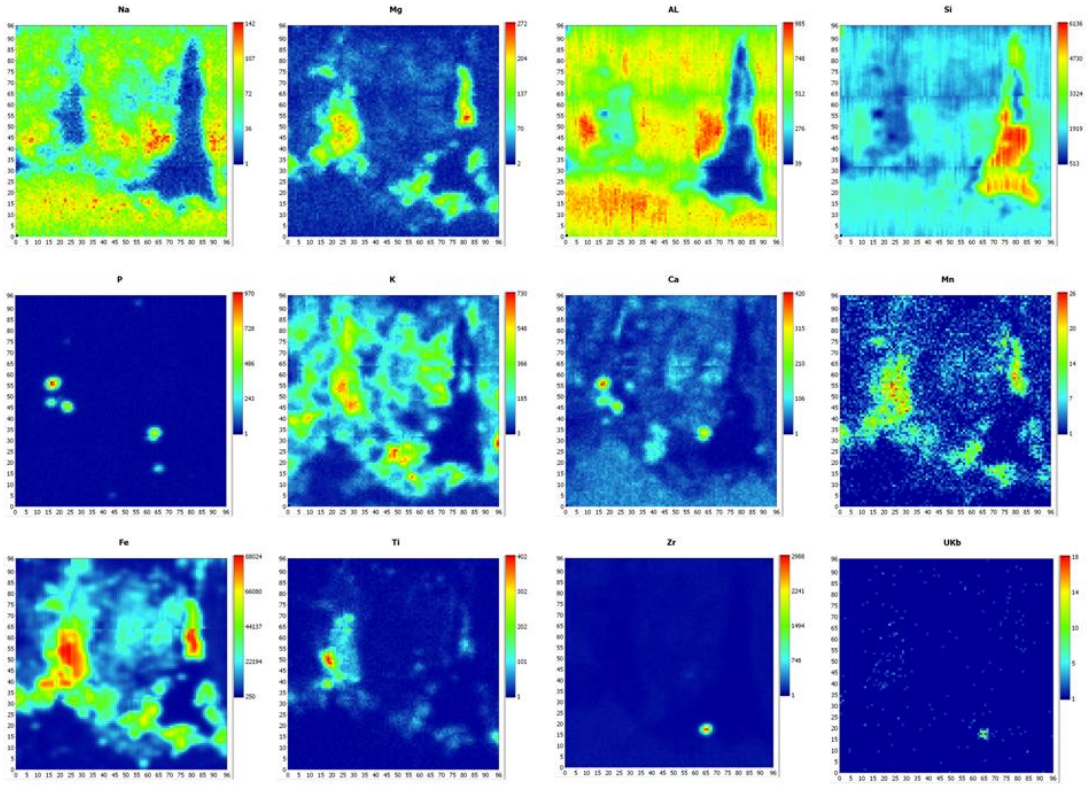

Figure 3. Elemental distribution maps obtained by µPIXE on an Aspö diorite sample with the new high-sensitivity AGLAE system.

The PIXE spectra in each area were deconvoluted assuming that all the elements were in oxide form and that the target was infinitely thick and the concentration sum was 100%. The four high energy spectra have always been added before deconvolution, but in several cases also individual high energy spectra were analyzed.

Table 2, presents the average concentration values measured on the studied Grimsel and Aspö samples, in comparison to values reported in the literature for both materials (Bradbury, 1989; Schäfer et al., 2012; Sundberg, 2002).

Table 2. Average elemental composition (weight %) obtained on Grimsel and Äspö rock by PIXE analyses carried out with the new AGLAE system, compared to values reported in the literature (Bradbury, 1989; Sundberg, 2002).

Sample		Grimsel	Grimsel [(Bradbury, 1989)	Aspo "fresh cut"	Aspo (Sundberg, 2002)
Na	%	5.15	4.1	7.34	4.55
Mg	%	0.19	0.5	1.45	1.76
Al	%	15.05	14	21.27	17.27
Si	%	72.48	71.8	61.04	62.71
P	%	0.04	0.1	0.33	0.24
S	%	0.08		0.07	
Cl	%	0.08		0.11	
K	%	4.74	4.2	1.77	3.05
Ca	%	0.61	1.6	3.05	3.75
Ti	%	0.10	0.3	0.22	0.66
Mn	%	0.04	0.07	0.05	0.08
Fe	%	1.07	2.2	2.6	6.9
Co	ppm				11
Ni	ppm	1.50		10	18
Cu	ppm	11.00		81	2
Zn	ppm	36.67		61	76
Ga	ppm	42.00		33	19
As	ppm	8.33			
Rb	ppm	372.00	700	105	
Sr	ppm	74.00	85	1163	1052
Y	ppm	102.00	126		22
Zr	ppm	13.00	250	36	168
Ba	ppm	403.00	650	1072	1162
La	ppm		175		
Pb	ppm	16.67		15	17
Th	ppm	21.00	24	20	9.5
U	ppm	42.00	8	9	4.4

The oxide composition has been obtained by combining the results of low and high energy detectors with an already established procedure (Zucchiatti et al., 2002). Taking advantage of the mapping capability (electrostatic + mechanical) and the high sensitivity of the detection system, we have selected map regions corresponding to specific minerals with MapPIXE acquisition and processing system (L.Pichon et al., 2010) and the corresponding PIXE spectra have been analyzed using the same procedure.

Composition obtained by μPIXE for both materials are in line those reported in the literature, although they are limited to small volumes. Main advantage of this technique is that, making use of the mapping facility, it is possible to select specific areas of the samples which are identified as rock constituent minerals (Figure 3), to identify elemental associations in the minerals.

B5. Conclusions

The μPIXE analyses carried out with the high-sensitivity micro-line of the AGLAE (Louvre Museum, France) allowed determining elemental composition in Rock samples form the Grimsel and Äspö hard rock underground research laboratories.

It was also possible to evaluate minimum detection limits for most elements in both rocks. These analyses facilitate the design of future colloid retention experiments. On one side they allow better selection of colloids (Au, CeO2, …amongst others)-

The selection of individual zones carried out in this work reduce the "effective" MDL, for example 12 times for La, 52 times for Th or 33 for U (Zucchiatti et al., In press).

Acknowledgment

The research leading to these results has received funding from EU FP7/2007-2011 under the grant agreements Nº 295487 (BELBAR, Bentonite Erosion: effects on the Long term performance of the engineered Barrier and Radionuclide Transport) and Nº 2620109 (ENSAR, European Nuclear Science and Applications Research). Prof. Zuchiatti and AGLAE experimental group are also greatly acknowledged.

References

Albarran, N., Missana, T., Garcia-Gutierrez, M., Alonso, U. and Mingarro, M., 2011. Strontium migration in a crystalline medium: effects of the presence of bentonite colloids. Journal of Contaminant Hydrology, 122(1-4): 76-85.

Alonso, U. et al., 2009. Quantification of Au nanoparticles retention on a heterogeneous rock surface. Colloids and Surfaces A: Physicochemical and Engineering Aspects, 347: 230-238.

Alonso, U., Missana, T., Patelli, A., Ravagnan, J. and Rigato, V., 2004. Experimental study of colloid interactions with rock surfaces, Scientific Basis for Nuclear Waste Management Xxviii. Materials Research Society Symposium Proceedings, pp. 461-466.

Alonso, U., Missana, T., Patelli, A., Rigato, V. and Ravagnan, J., 2007a. Colloid diffusion in crystalline rock: An experimental methodology to measure diffusion coefficients and evaluate colloid size dependence. Earth and Planetary Science Letters, 259(3-4): 372-383.

Alonso, U., Missana, T., Patelli, A., Rigato, V. and Ravagnan, J., 2007b. Colloid diffusion in crystalline rock: an experimental methodology to measure diffusion coefficients and evaluate colloid-size dependence. Earth and Planetary Science Letters, 259: 372-383.

Alonso, U., Missana, T., Patelli, A., Rigato, V. and Ravagnan., J., 2003. RBS and mPIXE analysis of uranium diffusion from the bentonite to the rock matrix in a deep geological waste disposal. Nuclear Instruments and Methods in Physics Research B,

207(2): 195-204.
Bradbury, M.H., Ed., 1989. Laboratory investigations in support of the migration experiments. Nagra techniocal Report 88-23. nagra, Switzerland. 88-23, NAGRA.
Campbell, J.L., Hopman, T.L., Maxwell, J.A. and Z.Nejedly, 2000. The Guelph PIXE software package III: Alternative proton database,. Nuclear Instruments and Methods in Physics Research B, 170: 193-204.
Fan, X. and Rowson, M.A., 2000. The efefct of $Pb(NO_3)_2$ on ilmenite flotation. Minerals Engineering, 13(2): 205-215.
Fornasiero, D. and Ralston, J., 2005. Cu(II) and Ni(II) activation in the f lotation of quartz, lizardite and chlorite. Int. J. Miner. Process., 76: 75-81.
Geckeis, H., 2008. Colloid influence on the radionuclide migration from a nuclear waste repository Geological Society, London, Special Publications 2004, 236:529-543;. Geological Society, London, Special Publications., 236: 529-543.
Huertas, F. et al., 2000. Full scale engineered barriers experiment for a deep geological repository for high-level radioactive waste in crystalline host rock. EC Final REPORT EUR 19147, EC Final REPORT EUR 19147.
James, S.C. and Chrysikopoulos, C.V., 1999. Transport of polydispersed colloid suspensions in a single fracture. Water Resources Research, 35(3): 707-718.
KIT-INE, 2011. Provision of new fracture bearing drill core samples obtained, handled, transported and stored under anoxic conditions, including first documentation. CROCK Project DELIVERABLE (D-N°:1.1).
Kosakowsky, G., 2004. Anomalous transport of colloids and solutes in a shear zone. Journal of Contaminant Hydrology, 72(1-4): 23-46.
L.Pichon, Beck, L., Walter, P., Moignard, B. and Guillou, T., 2010. A new mapping acquisition and processing system for simultaneous PIXE-RBS analysis with external beam,. Nuclear Instruments and Methods in Physics Research B, 268: 2028-2033.
Leskinen, A. et al., 2007. Determination of granites' mineral specific porosities by PMMA method and FESEM/EDAX. In Scientific Basis for Nuclear Waste Management XXX, edited by D.S. Dunn, C. Poinssot, B. Beg. Mater. Res. Soc. Symp. Proc. 985, 0985-NN11-20,Warrendale, PA., Scientific Basis for Nuclear Waste Management. Materials Research Society, Boston, USA:.
Missana, T., Alonso, U., Albarran, N., Garcia-Gutierrez, M. and Cormenzana, J.-L., 2011. Analysis of colloids erosion from the bentonite barrier of a high level radioactive waste repository and implications in safety assessment. Physics and Chemistry of the Earth, 36(17-18): 1607-1615.
Missana, T., Alonso, U., Garcia-Gutierrez, M. and Mingarro, M., 2008a. Role of bentonite colloids on europium and plutonium migration in a granite fracture. Applied Geochemistry, 23(6): 1484-1497.
Missana, T., Alonso, U., García-Gutiérrez, M. and Mingarro, M., 2008b. Role of bentonite colloids on europium and plutonium migration in a granite fracture. Applied Geochemistry, 23(6): 1484-1497.
Moignard, B. et al., 2012. "New AGLAE" project: a new PIXE-RBS-IBIL multi detector designed and installed on an external beam, SNEAP 2012, Legnaro, Italy.
Möri, A. et al., 2003. The colloid and radionuclide retardation experiment at the Grimsel Test Site: influence of bentonite colloids on radionuclide migration in fractured rock. Colloids and Surfaces A, 217: 33-47.
Patelli, A., Alonso, U., Rigato, V., Missana, T. and Restello, S., 2006. Validation of the RBS analysis of colloid migration through a rough granite surface. Nuclear Instruments and Methods in Physics Research B, 249: 575-578.

Pichon, L., Beck, L., Walter, P., Moignard, B. and Guillou, T., 2010. A new mapping acquisition and processing system for simultaneous PIXE-RBS analysis with external beam,. Nuclear Instruments and Methods in Physics Research B, 268: 2028-2033.

Schaefer, T. et al., 2012. Nanoparticles and their influence on radionuclide mobility in deep geological formations. Applied Geochemistry, 27(2): 390-403.

Schäfer, T., Geckeis, H., Bouby, M. and Fanghänel, T., 2004. U, Th, Eu and colloid mobility in a granite fracture under near-natural flow conditions. Radiochimica Acta, 92(9-11).

Schäfer, T., Satge, E., Büchner, S., Huber, F. and G¡Drake, H., 2012. Characterization of new crystalline material for investigations within CP CROCK. 1st Workshop Proceedings of the CP - "Crystalline Rock retention processes" (7th EC FP CP CROCK). KIT Scientific Reports 7629 [ISBN 978-3-86644-925-1] pp. 63-72.

Song, L. and Elimelech, M., 1993. Dynamics of colloid deposition in porous media: Modelling the role of retained particles. Colloids and Surfaces A, 73: 49-63.

Sundberg, J., 2002. Determination of thermal properties at Äspö HRL. Comparison and evaluation of methods and methodologies for borehole KA 2599 G01. SKB Report R-02-27, Sweden.

Zucchiatti, A. et al., In press. Detection of actinides and rare earths in natural matrices with the AGLAE new, high sensitivity detection set-up. Nuclear Instruments and Methods in Physics Research Section B: Beam Interactions with Materials and Atoms.

Zucchiatti, A. et al., 2002. PIXE and -PIXE analysis of glazes from terracotta sculptures of the della Robbia workshop. Nuclear Instruments and Methods in Physics Research B, 189: 358-363.